

STRUCTURE NOTE

Structure of a putative BenF-like porin from *Pseudomonas fluorescens* Pf-5 at 2.6 Å resolution

Parthasarathy Sampathkumar,^{1*} Frances Lu,¹ Xun Zhao,¹ Zhenzhen Li,¹ Jeremiah Gilmore,¹ Kevin Bain,¹ Marc E. Rutter,¹ Tarun Gheyi,¹ Kenneth D. Schwinn,¹ Jeffrey B. Bonanno,² Ursula Pieper,^{3,4,5} J. Eduardo Fajardo,^{2,6} Andras Fiser,^{2,6} Steven C. Almo,² Subramanyam Swaminathan,⁷ Mark R. Chance,⁸ David Baker,⁹ Shane Atwell,¹ Devon A. Thompson,¹ J. Spencer Emtage,¹ Stephen R. Wasserman,¹⁰ Andrej Sali,^{3,4,5} J. Michael Sauder,¹ and Stephen K. Burley¹

¹ New York SGX Research Center for Structural Genomics (NYSGXRC), Eli Lilly and Company, Lilly Biotechnology Center, San Diego, California 92121

² Department of Biochemistry, Albert Einstein College of Medicine, Bronx, New York 10461

³ Department of Bioengineering and Therapeutic Sciences, University of California, San Francisco, California 94158

⁴ Department of Pharmaceutical Chemistry, University of California, San Francisco, California 94158

⁵ California Institute for Quantitative Biosciences, University of California, San Francisco 94158

⁶ Department of Systems and Computational Biology, Albert Einstein College of Medicine, Bronx, NY 10461

⁷ Department of Biology, Brookhaven National Laboratory, Upton, New York 11973

⁸ Department of Physiology and Biophysics, Center for Proteomics and Bioinformatics, Case Western Reserve University, Cleveland, Ohio 44106

⁹ Department of Biochemistry, University of Washington, Seattle, Washington 98195

¹⁰ LRL-CAT, Eli Lilly and Company, Advanced Photon Source, Argonne National Laboratory, Argonne, Illinois 60439

Key words: BenF-like; substrate-specific porin; OprD superfamily; OprD subfamily; OpdK subfamily; benzoate; *Pseudomonas*; integral membrane protein.

INTRODUCTION

Gram-negative bacteria typically overcome poor permeability of outer membranes through general porins like OmpF and OmpC, which form water-filled transmembrane pores permitting diffusion of hydrophilic molecules with no particular selectivity.¹ Many bacteria lacking such general porins use substrate-specific porins to overcome growth-limiting conditions and facilitate selective transport of metabolites. Exclusive reliance on substrate-specific porins yields lower membrane permeability to small molecules (<600 Da) versus that seen for *Escherichia coli*. In *Pseudomonads*, transit of most small molecules across the cell membrane is thought to be mediated by substrate-specific channels of the OprD superfamily.² This property explains, at least in part, the high incidence of *Pseudomonas aeruginosa* antibiotic resistance. High-throughput DNA sequencing of the *P. aeruginosa* chromosome revealed the presence of 19 genes encoding structur-

ally related, substrate-specific porins (with 30–45% pairwise amino acid sequence identity) that mediate transmembrane passage of small, water-soluble compounds. The OprD superfamily encompasses the eponymous OprD subfamily, which includes 9 *P. aeruginosa* proteins that convey basic amino acids and carbapenem antibiotics,³ and the OpdK subfamily, which includes 11 *P. aeruginosa* proteins that convey aromatic acids and other small aromatic compounds.⁴ Genome sequencing of other gram-negative bacteria has revealed addi-

Additional Supporting Information may be found in the online version of this article. Grant sponsor: NIH; Grant number: U54 GM074945, NIH R01 GM54762; Grant sponsor: U.S. Department of Energy, Office of Basic Energy Sciences

*Correspondence to: Parthasarathy Sampathkumar, Eli Lilly and Company, 10300 Campus Point Drive, Suite 200, San Diego, CA 92121.

E-mail: sampathkumarpa@lilly.com

Received 9 May 2010; Accepted 26 June 2010

Published online 23 July 2010 in Wiley Online Library (wileyonlinelibrary.com).

DOI: 10.1002/prot.22829

tional members of the OprD and OpdK subfamilies in various organisms, including other pseudomonads. Among the many bacteria in which OprD superfamily members have been identified are *P. putida*, *P. fluorescens* Pf-5, *P. syringae*, and *Azotobacter vinelandii*, all of which share closely related genes that encode the so-called BenF-like porins. In *P. putida*, *benF* is part of an operon involved in benzoate catabolism regulated by *benR*.⁵ Within this operon, *benK*, *benE*, and *benF* genes have been suggested to contribute toward either influx or efflux of benzoate.^{5,6} BLAST⁷ analysis of the amino acid sequence of *P. fluorescens* Pf-5 gene PFL1329 (Uniprot⁸ id: <http://www.uniprot.org/uniprot/Q4KH25>)⁹ against *P. putida* KT2440 strain¹⁰ identified 20 related porins. The top six hits include *P. putida* KT2440 genes PP1383 (annotated as BenF-like), PP2517 (annotated as BenF-like), and PP3168 (annotated as BenF), which share sequence identities of 76%, 66%, and 44% with PFL1329, respectively. The precise functions of these genes are not yet known. Therefore, we refer to the protein product of gene PFL1329 as PflBenF-like, which reflects its current annotation in the Uniprot database.

Crystal structures of OprD¹¹ and OpdK (vanillate specific porin),¹² both from *P. aeruginosa* (designated below as PaOprD and PaOpdK, respectively) have been determined. Herein, we report the crystal structure of a putative BenF-like porin from *P. fluorescens* Pf-5 (PflBenF-like). For the sake of brevity, all subsequent references to the PflBenF-like porin will be made using PflBenF. X-ray crystallography revealed a canonical 18-stranded β -barrel fold that forms a central pore with a diameter of ~ 4.6 Å. We describe detailed comparisons of the PflBenF structure with those of PaOprD and PaOpdK.

METHODS

Cloning and expression of PflBenF

The gene encoding putative *P. fluorescens* BenF-like porin was cloned from genomic DNA of the strain Pf-5 (American Type Culture Collection, USA). The desired truncation (encoding residues 30–420) was PCR amplified using GAGTCGGGCTTTCTCGAAGATGC and CCAGCAGGCTGAGGGGATAGC as forward and reverse primers, respectively. The purified PCR product was subsequently TOPO[®] (Invitrogen, USA) cloned into pSGX3, a derivative of pET26b(+), giving rise to a fusion protein with a noncleavable C-terminal hexa-histidine tag. Plasmids were transfected into BL21(DE3)-Condon+RIL (Invitrogen) cells for overexpression. Expression was carried out at 22°C in 4 L of Terrific Broth¹³ supplemented with kanamycin (50 μ g/mL) and chloramphenicol (35 μ g/mL). Protein expression was induced by addition of 0.4 mM IPTG at an OD₆₀₀ of 1.0. Cells were harvested after 21 h by centrifugation at 4°C. Virtually, all PflBenF protein was found in inclusion bodies.

Purification and refolding of PflBenF

The *E. coli* cell pellet was resuspended in 30 mL of cold buffer (20 mM Tris–HCl pH 8.0, 500 mM NaCl, 25 mM imidazole, and 0.1% Tween 20), and cells were lysed via sonication. Inclusion bodies were pelleted by centrifugation at 4°C and solubilized in 20 mM Tris–HCl pH 8.0, 1 mM β -mercaptoethanol, and 6M guanidinium chloride. Solubilized PflBenF was purified under denaturing conditions via immobilized metal ion affinity chromatography with NiNTA resin by washing the column with solubilization buffer plus 50 mM imidazole. Following elution with the solubilization buffer plus 400 mM imidazole, PflBenF was diluted to a concentration of ~ 1 mg/mL and refolded by drop wise dilution into a buffer containing 20 mM Tris–HCl pH 8.0, 150 mM NaCl, 0.5 mM TCEP, and 0.5% (w/v) lauryldimethylamineoxide (LDAO) to a final protein concentration of ~ 250 μ g/mL. The refolded protein was concentrated by immobilization on NiNTA resin followed by elution with 20 mM Tris–HCl pH 8.0, 200 mM NaCl, 10% (v/v) glycerol, 0.5 mM TCEP, 5 mM LDAO, and 400 mM imidazole. Refolded PflBenF was further purified by size exclusion chromatography using a 120 mL Superdex S200 column equilibrated with 20 mM Tris–HCl pH 8.0, 200 mM NaCl, 10% (v/v) glycerol, 0.5 mM TCEP, and 5 mM LDAO. SDS–PAGE analysis showed greater than 95% purity and protein fractions corresponding to the symmetric portion of the size exclusion chromatography profile were pooled and concentrated using spin filters. Size exclusion chromatography with multiangle laser light scattering (SEC-MALLS) revealed PflBenF to be a monomer associated with one LDAO micelle (data not shown).

Crystallization, data collection, and structure determination

PflBenF (protein concentration ~ 9.0 mg/mL; 0.3- μ L protein-containing solution + 0.3- μ L reservoir solution) was subjected to crystallization screening with the Classics, Classics II, CompAS, and PEG kits (Qiagen, USA) using a Phoenix Liquid Handling System (Art Robbins Instruments, USA) via sitting drop vapor diffusion at 4 and 21°C. Several conditions yielded thin needles and microcrystals. Subsequent optimization was performed with additive and detergent screening. A single crystal diffracting to ~ 2.6 Å resolution was obtained with 21% PEG 3350, 100 mM citrate, and 10% (w/v) ANAPOE-X-114 (from the detergent screen) at 21°C. Diffraction data were recorded under standard cryogenic conditions using the LRL-CAT 31-ID beamline at the advanced photon source and processed with MOSFLM¹⁴ and SCALA (Collaborative Computing Project Number 4, 1994).¹⁵ A polyalanine model of PaOpdK was used for molecular replacement with PHASER¹⁶ as implemented in CCP4. The atomic model of PflBenF was built manually by visual inspection with COOT¹⁷ and refined to convergence using REFMAC5¹⁸ (Table I). Structural

Table 1
Crystallographic Data Collection and Refinement Statistics for PflBenF

Data collection	
PDB code	3JTY
Space group	$P2_1$
Unit-cell dimensions (Å, °)	$a = 62.1, b = 210.6,$ $c = 84.1, \beta = 97.8$
Resolution (Å)	53.68–2.58 (2.72–2.58) ^a
Number of unique reflections	67,053 (9774)
Completeness (%)	100.0 (100.0)
R_{sym} (%)	14.0 (52.7)
Multiplicity	3.9 (3.8)
$\langle I/\sigma(I) \rangle$	6.1 (2.7)
Refinement	
Resolution (Å)	35.11–2.58
R -factor (%)	22.0
R_{free} (%)	27.5
Number of nonhydrogen atoms	
Protein	11,859
Ligands	32
Water molecules	25
Average B-factors (Å²)	
Protein	41.9
Ligands	75.4
Water molecules	35.2
RMS deviations from ideal values	
Bond length (Å)	0.018
Bond angles (°)	1.60
Ramachandran plot ¹⁹	
MolProbity ²⁰ residues in favored region (%)	95.6
Allowed region (%)	99.9

^aValues in parenthesis correspond to highest-resolution shell.

analyses were carried out using COOT and CCP4, and illustrations were prepared using PyMol (<http://pymol.sourceforge.net>).

RESULTS AND DISCUSSION

Overall structure of PflBenF-like porin

An N-terminal truncation of the putative BenF-like porin from *P. fluorescens Pf-5* (PflBenF, residues 30–420) was overexpressed in *E. coli*, purified under denaturing conditions from inclusion bodies by immobilized metal ion affinity chromatography, refolded by dilution into a buffer containing LDAO, and further purified by size exclusion chromatography. PflBenF crystallized in the monoclinic space group $P2_1$ with four molecules in the asymmetric unit (Table 1). The PflBenF polypeptide chain could be continuously traced for one protomer (denoted chain A and used for all illustrations and analyses herein). In each of chains B, C, and D, residues 112–115 were disordered in the experimental electron density map and could not be modeled. Otherwise, the structures of the four protomers are very similar [pairwise root mean square deviations (r.m.s.d.s) range from 0.31 to 0.39 Å for common α -carbon atomic pairs].

PflBenF adopts the canonical β -barrel porin fold consisting of 18 antiparallel β -strands arranged in a cylinder [Fig. 1(A,B)]. Pairwise comparisons of the structure of PflBenF with those of PaOpdK and PaOprD using SSM²⁴ revealed highly similar polypeptide chain folds (PflBenF vs. PaOpdK: r.m.s.d. = 0.9 Å, sequence identity = 53% for 369 α -carbon pairs; PflBenF vs. PaOprD: r.m.s.d. = 1.3 Å, sequence identity = 40% for 342 α -carbon pairs; PaOpdK vs. PaOprD: r.m.s.d. = 1.3 Å, sequence identity = 39% for 382 α -carbon pairs). The β -strands of PflBenF are connected by shorter turns T1–T8 and longer loops L1–L7 on the periplasmic and extracellular faces of the barrel, respectively. Loops L3 and L7 fold into the interior of the β -barrel, where they help define the geometry of the pore [Fig. 1(B)]. As for PaOpdK and PaOprD, PflBenF also possesses short S5 and S6 β -strands, which are characteristic of porins that form trimers in the outer membrane.²⁵ Notwithstanding this similarity, PflBenF protomers do not make extensive intermolecular interactions within the crystal lattice. Recombinant forms of both PaOpdK and PaOprD also appear monomeric in the crystal lattice. However, recombinant PaOpdK inserted into artificial lipid bilayer oligomerizes and behaves as a trimeric ion-conductor.¹¹ Given the short lengths of the S5 and S6 β -strands in the PflBenF-like porin and the PaOpdK precedent, there is no compelling reason to believe that PflBenF functions as a monomer.

Structure of the PflBenF benzoate-specific channel

The structure of the PflBenF β -barrel revealed a quasi-circular pore [Fig. 1(B)] with a diameter of ~ 4.6 Å (as estimated with HOLE²¹). Sequence alignment of PflBenF, *P. putida* BenF, PaOpdK, PaOprD, and three other porins with various annotations (pairwise sequence identities with PflBenF ranging from 34 to 76%) revealed significant conservation for β -strand residues [Fig. 1(C)] and those within the loops L2, L3, and L7. The electrostatic properties of the periplasmic and extracellular faces of PflBenF are illustrated in Figure 1(D). On the periplasmic face, conserved basic and nonpolar surface features are visible in the immediate vicinity of channel constriction. There is no corresponding concentration of polar surface features on the extracellular side of the channel immediately beyond the constriction. In fact, the extracellular face of the protein is largely devoid of polar features [Fig. 1(D), lower panel]. The entire periplasmic face of PflBenF is also considerably more polar than the extracellular face of the protein.

Evidence for an aromatic acid selectivity filter shared by PflBenF and *P. aeruginosa* OpdK

The pore constriction of PflBenF is lined by residues Asp151 and Arg154 from loop L3; Ser310, Asp317,

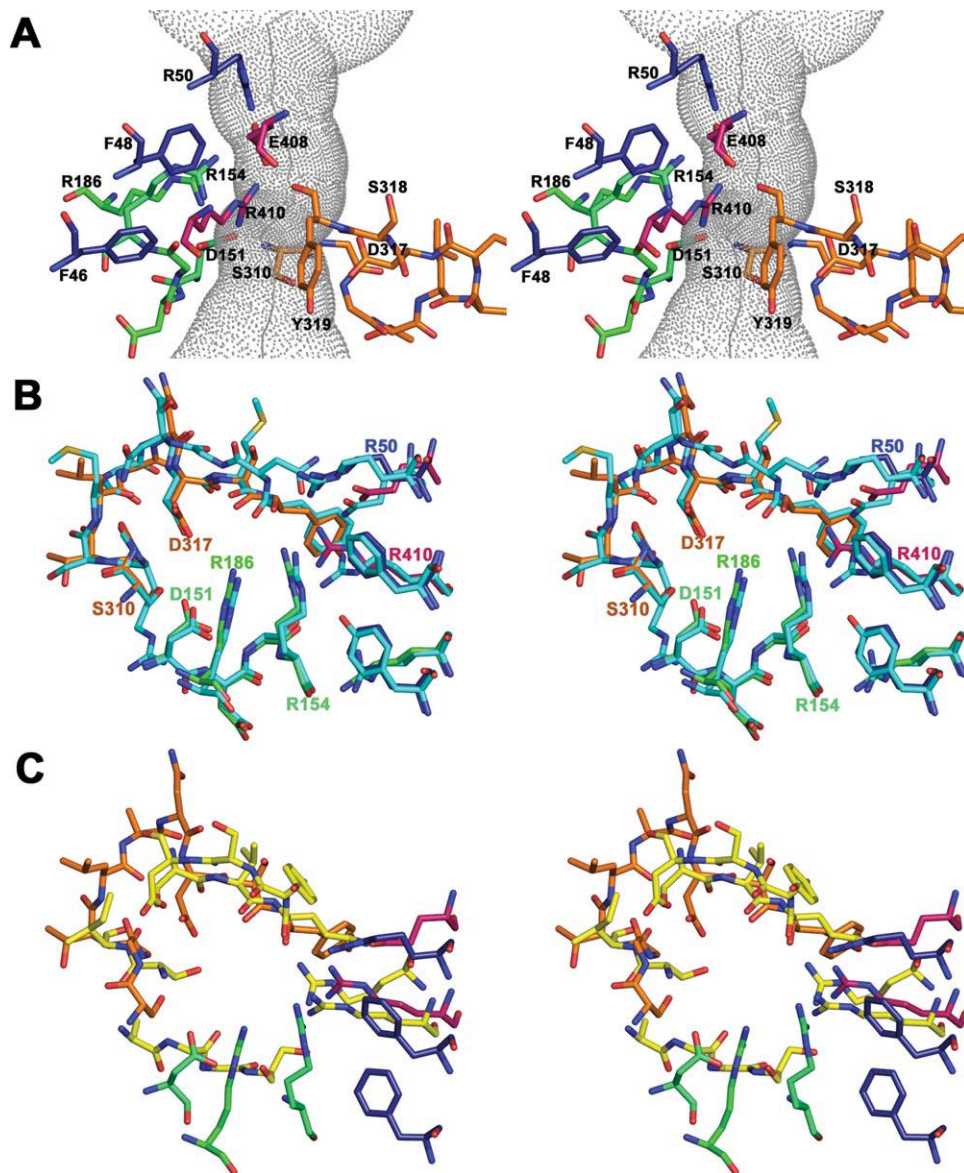


Figure 2

Structure of a putative aromatic acid selectivity filter. **A:** Atomic stick figure representation of the PflBenF pore forming residues surrounding the dot surface of the pore²¹ viewed parallel to the cell membrane (carbon atoms color coded to correspond to the representation in Figure 1(A): blue denotes β 1, green denotes L3 and L4, light brown denotes L7, pink denotes β 10; nitrogen atoms-blue; oxygen atoms-red). **B:** Stereoview overlay of selected pore forming residues of PflBenF with residues defining the aromatic acid selectivity pore [color coded as in Fig. 2(A), labeled with PflBenF sequence numbering] and *P. aeruginosa* OpdK (carbon atoms color coded cyan). **C:** Stereoview overlay of selected pore forming residues of PflBenF [color coded as in Fig. 2(A)] and *P. aeruginosa* OprD (carbon atoms color-coded yellow).

Ser318, and Tyr319 from loop L7; Phe46, Phe48, and Arg50 from the S1 β -strand; Arg186 from loop L4; and Glu408 and Arg410 from the S18 β -strand [Fig. 2(A)]. These four Arg residues decorate the periplasmic lip of the pore giving rise to a discrete positively charged patch between 4 and 6 o'clock [Fig. 1(D), upper panel]. Of these 12 pore forming residues, four arginines and an aspartate at position 317 are invariant among the six divergent sequences included in Figure 1(C). In addition, Asp151 and Ser310 are highly conserved.

Given that PflBenF and PaOpdK are thought to transport chemically similar substrates (putative benzoate selectivity versus experimentally confirmed vanillate uptake), it is not unexpected that their respective pore constrictions are essentially identical in size (diameters of ~ 4.6 and ~ 4.4 Å, respectively) and shape [Fig. 2(B)]. What is surprising, however, is the finding that the seven pore forming residues with side chains that contribute directly to the constriction (or selectivity filter) are identical between PflBenF and PaOpdK [Figs. 1(C) and

2(B)]. Specifically, Arg50 (*Arg22*, italics denotes PaOprD residues), Asp151 (*Asp123*), Arg154 (*Arg126*), Arg186 (*Arg158*), Ser310 (*Ser282*), Asp317 (*Asp289*), and Arg410 (*Arg381*) are invariant between these two porins [Figs. 1(C) and 2(B)]. The only notable difference is the side-chain conformation of Arg410, which brings its guanidinium group closer to the constriction in the case of PflBenF. In contrast, the PaOprD pore constriction is smaller than that of PflBenF and PaOprK (~ 3.7 Å vs. ~ 4.5 Å), differs in shape, and is defined by a different configuration of selectivity filter residues [Fig. 2(C)]. Thus, the selectivity determining residues of the vanillate and putative benzoate pores appear to be similar. Further characterization of the function of PflBenF and other porins sharing this sequence motif will be required to establish whether or not it is in fact a signature of aromatic acid channels.

One of the metrics guiding target selection in structural genomics is modeling leverage at the level of greater than 30% sequence identity (see Supporting Information Methods).^{26,27} Searching of the UniProtKB database of all known protein sequences using the sequences of PflBenF, PaOprK, and PaOprD identified 221 unique protein sequences with sequence identity greater than 30% to at least one of these three proteins. The inaugural structure of PaOprD, enabled modeling of 165 related proteins (Supporting Information Fig. S1). Subsequent determination of the structure of PaOprK enabled homology modeling of an additional three protein sequences. In contrast, determination of the PflBenF structure enabled homology modeling of 53 additional protein sequences (Supporting Information Fig. S1). Thus, the structure of PflBenF, reported herein, expands significantly the number of homology models of OprD and OprK family of substrate-specific porins. Experimental structures of additional OprD/OprK subfamily members should provide useful guides for planning experiments aimed at defining the mechanisms governing pore selectivity.

ACKNOWLEDGMENTS

Access to the LRL-CAT beam-line facilities at Sector 31 of the advanced photon source was provided by Eli Lilly and Company, which operates the facility. Use of the Advanced Photon Source was supported by the U.S. Department of Energy, Office of Science, Office of Basic Energy Sciences, under Contract No. DE-AC02-06CH11357. Atomic coordinates and structure factors of PflBenF were deposited to the PDB (www.rcsb.org) on 14 September 2009 with PDB accession code 3JTY. The NYSGXRC target identifier for PflBenF in TargetDB (<http://targetdb.pdb.org>) is "NYSGXRC-10383p." Expression clone sequences and selected interim experimental results are available in PepcDB (<http://pepcdb.pdb.org/>).

REFERENCES

- Nikaido H. Molecular basis of bacterial outer membrane permeability revisited. *Microbiol Mol Biol Rev* 2003;67:593–656.
- Hancock RE, Brinkman FS. Function of pseudomonas porins in uptake and efflux. *Annu Rev Microbiol* 2002;56:17–38.
- Trias J, Nikaido H. Protein D2 channel of the *Pseudomonas aeruginosa* outer membrane has a binding site for basic amino acids and peptides. *J Biol Chem* 2006;265:15680–15684.
- Tamber S, Ochs MM, Hancock RE. Role of the novel OprD family of porins in nutrient uptake in *Pseudomonas aeruginosa*. *J Bacteriol* 2006;188:45–54.
- Cowles CE, Nichols NN, Harwood CS. BenR, a XylS homologue, regulates three different pathways of aromatic acid degradation in *Pseudomonas putida*. *J Bacterol* 2000;182:6339–6346.
- Nishikawa Y, Yasumi Y, Noguchi S, Sakamoto H, Nikawa J. Functional analyses of *Pseudomonas putida* benzoate transporters expressed in the yeast *Saccharomyces cerevisiae*. *Biosci Biotechnol Biochem* 2008;72:2034–2038.
- Altschul SF, Madden TL, Schaffer AA, Zhang J, Zhang Z, Miller W, Lipman DJ. Gapped BLAST and PSI-BLAST: a new generation of protein database search programs. *Nucleic Acids Res* 1997;25:3389–3402.
- The UniProt Consortium. The universal protein resource (UniProt) in 2010. *Nucleic Acids Res* 2010;38(Database issue):D142–D148.
- Paulsen IT, Press CM, Ravel J, Kobayashi DY, Myers GS, Mavrodi DV, De Boy RT, Seshadri R, Ren Q, Madupu R, Dodson RJ, Durkin AS, Brinkac LM, Daugherty SC, Sullivan SA, Rosovitz MJ, Gwinn ML, Zhou L, Schneider DJ, Cartinhour SW, Nelson WC, Weidman J, Watkins K, Tran K, Khouri H, Pierson EA, Pierson LS, III, Thomashow LS, Loper JE. Complete genome sequence of the plant commensal *Pseudomonas fluorescens Pf-5*. *Nat Biotechnol* 2005;23:873–878.
- Nelson KE, Weinel C, Paulsen IT, Dodson RJ, Hilbert H, Martins dos Santos VA, Fouts DE, Gill SR, Pop M, Holmes M, Brinkac L, Beanan M, DeBoy RT, Daugherty S, Kolonay J, Madupu R, Nelson W, White O, Peterson J, Khouri H, Hance I, Chris Lee P, Holtzapfle E, Scanlan D, Tran K, Moazzez A, Utterback T, Rizzo M, Lee K, Kosack D, Moestl D, Wedler H, Lauber J, Stjepandic D, Hoheisel J, Straetz M, Heim S, Kiewitz C, Eisen JA, Timmis KN, Dusterhöft A, Tümmeler B, Fraser CM. Complete genome sequence and comparative analysis of the metabolically versatile *Pseudomonas putida* KT2440. *Environ Microbiol* 2002;4:799–808.
- Biswas S, Mohammad MM, Patel DR, Movileanu L, van den Berg B. Structural insight into OprD substrate specificity. *Nat Struct Mol Biol* 2007;14:1108–1109.
- Biswas S, Mohammad MM, Movileanu L, van den Berg B. Crystal structure of the outer membrane protein OprD from *Pseudomonas aeruginosa*. *Structure* 2008;16:1027–1035.
- Sambrook J, Fritsch EF, Maniatis T. *Molecular cloning: a laboratory manual*, 2nd ed. Cold Spring Harbour, NY: Cold Spring Harbour Laboratory; 1989.
- Leslie AGW, Brick P, Wonacott AJ. An improved program package for the measurement of oscillation photographs. *CCP4 News Lett* 1986;18:33–39.
- Collaborative Computing Project Number 4. The CCP4 suite: programs for protein crystallography. *Acta Crystallog Sect D Biol Crystallogr* 1994;50:760–763.
- McCoy AJ, Grosse-Kunstleve RW, Adams PD, Winn MD, Storoni L, Read RJ. Phaser crystallographic software. *J Appl Cryst* 2007;40:658–674.
- Emsley P, Cowtan K. COOT: model-building tools for molecular graphics. *Acta Crystallogr Sect D Biol Crystallogr* 2004;60:2126–2132.
- Murshudov GN, Vagin AA, Dodson EJ. Refinement of macromolecular structures by the Maximum-Likelihood Method. *Acta Crystallogr D Biol Crystallogr* 1997;53:240–255.

19. Ramakrishnan C, Ramachandran GN. Stereochemical criteria for polypeptide and protein chain conformations. II. Allowed conformations for a pair of peptide units. *Biophys J* 1965;5:909–933.
20. Davis IW, Leaver-Fay A, Chen VB, Block JN, Kapral GJ, Wang X, Murray LW, Arendall WB, III, Snoeyink J, Richardson JS, Richardson DC. Mol Probity: all-atom contacts and structure validation for proteins and nucleic acids. *Nucl Acids Res* 2007;35:W375–W383.
21. Smart OS, Neduvilil JG, Wang X, Wallace BA, Sansom MSP. HOLE: a program for the analysis of the pore dimensions of ion channel structural models. *J Mol Graph* 1996;14:354–360.
22. Larkin MA, Blackshields G, Brown NP, Chenna R, McGettigan PA, McWilliam H, Valentin F, Wallace IM, Wilm A, Lopez R, Thompson JD, Gibson TJ, Higgins DG. ClustalW and ClustalX version 2. *Bioinformatics* 2007;23:2947–2948.
23. Gouet P, Courcelle E, Stuart DI, Metz F. ESPript: multiple sequence alignments in PostScript. *Bioinformatics* 1999;15:305–308.
24. Krissinel E, Henrick K. Secondary-structure matching (SSM), a new tool for fast protein structure alignment in three dimensions. *Acta Crystallogr D Biol Crystallogr* 2004;60:2256–2268.
25. Schulz GE. The structure of bacterial outer membrane proteins. *Biochim Biophys Acta* 2002;1565:308–317.
26. Eswar N, John B, Mirkovic N, Fiser A, Ilyin VA, Pieper U, Stuart AC, Marti-Renom MA, Madhusudhan MS, Yerkovich B, Sali A. Tools for comparative protein structure modeling and analysis. *Nucleic Acids Res* 2003;31:3375–3380.
27. Pieper U, Eswar N, Webb BM, Eramian D, Kelly L, Barkan DT, Carter H, Mankoo P, Karchin R, Marti-Renom MA, Davis FP, Sali A. MODBASE, a database of annotated comparative protein structure models and associated resources. *Nucleic Acids Res* 2009;37:D347–354.